

## Effect of Carboxymethyl Cellulose Concentration on Structural, Morphological and Magnetic Properties of Barium Hexaferrite: A Study Based on Sol-Gel Auto-Combustion Method

PARINTIP RATTANABURI<sup>1,✉</sup>, PAWEENA PORRAWATKUL<sup>2,✉</sup>, NONGYAO TEPPAYA<sup>2,✉</sup>, AMNUAY NOYPHA<sup>3,✉</sup>,  
RUNGNAPA PIMSEN<sup>2,✉</sup>, SAKSIT CHANTHAI<sup>4,✉</sup> and PRAWIT NUENGMATCHA<sup>1,2,\*✉</sup>

<sup>1</sup>Creative Innovation in Science and Technology, Faculty of Science and Technology, Nakhon Si Thammarat Rajabhat University, Nakhon Si Thammarat 80280, Thailand

<sup>2</sup>Nanomaterials Chemistry Research Unit, Department of Chemistry, Faculty of Science and Technology, Nakhon Si Thammarat Rajabhat University, Nakhon Si Thammarat 80280, Thailand

<sup>3</sup>Department of Physics, Faculty of Education, Nakhon Si Thammarat Rajabhat University, Nakhon Si Thammarat 80280, Thailand

<sup>4</sup>Materials Chemistry Research Center, Department of Chemistry and Center of Excellence for Innovation in Chemistry, Faculty of Science, Khon Kaen University, Khon Kaen 40002, Thailand

\*Corresponding author: Tel/Fax: +66 7 5377443; E-mail: [pnuengmatcha@gmail.com](mailto:pnuengmatcha@gmail.com)

Received: 3 October 2021;

Accepted: 14 December 2021;

Published online: 20 April 2022;

AJC-20760

This study was intended to assess the role of carboxymethyl cellulose (CMC) as a chelating agent in the synthesis of barium hexaferrite ( $\text{BaFe}_{12}\text{O}_{19}:\text{BaF}$ ). The effect of varying concentrations of CMC was studied *via* the sol-gel auto-combustion method following the requirements of green chemistry synthesis. The formation of BaF nanoparticles was confirmed using XRD, SEM, EDS, VSM, FTIR and UV-Vis-DRS techniques. The characterized XRD peak indicates the formation of good quality crystalline samples at 6% (w/v) of CMC concentration. SEM analysis suggested that the synthesized BaF is spherical, with sizes ranging from 10-15 nm. The M-H hysteresis loops obtained for the samples showed their soft and hard magnetic behaviour. With the increasing CMC concentration, magnetism becoming harder and an increase in the  $M_s$  value can be observed. The UV-Vis-DRS techniques revealed that the band gap energy of synthesized BaF increased with an increase in the concentration of CMC.

**Keywords:** Carboxymethyl cellulose, Barium hexaferrite, Green synthesis.

### INTRODUCTION

Barium hexaferrite (BaF,  $\text{BaFe}_{12}\text{O}_{19}$ ) can be considered as a possible candidate for preparing a nanocomposite material. BaF has good chemical stability and corrosion resistance in addition to its high saturation magnetization and coercive forces [1]. Furthermore, nanostructured BaF is a promising material for high-capacitive memory and high-frequency microwave devices [2]. The realization of such a well-organized nanostructure will be based on the availability of high-quality raw materials, which should constitute a magnetic domain and a narrow distribution of particles. Several techniques have been designed for the efficient synthesis of BaF, including the reverse microemulsion process [3], co-participation, hydrothermal procedure [4], sol-gel route [5,6] and sol gel-auto combustion

[7]. Among these methods, sol-gel auto combustion is attractive because it requires only low temperatures for the combustion process. The procedure involved is relatively easy and thus, the cost of the sol-gel auto combustion is lower when compared with other techniques. These advantages have prompted many researchers to adopt this method for preparing BaF. There are reports on the synthesis of BaF nanoparticles *via* different methods using glycine, citric acid [8] and urea as chelating agents [9]. It must be magnetically characterized as a mole for a single phase and Fe:Ba ratio should be appropriate. If the barium quantity used is less,  $\text{Fe}_2\text{O}_3$  would be produced during the stoichiometry cleaning stage due to an excessive amount of Fe and if an excess of barium is used,  $\text{BaFe}_2\text{O}_4$  will be generated in the intermediate stage [10]. For the majority of  $\text{BaFe}_{12}\text{O}_{19}$  impurity and intermediate powder produced, the magnetic

properties will be poor. Temperature sintering has a significant influence in determining the barium hexaferrite formation and the suitable particulate size reactivity. The value of responsibility is also affected by the sintering temperature [11].

Green synthesis research on nanomaterials through the use of natural biomaterials like plants and flora is considered as a new nanotechnology branch known as “microorganisms in green synthesis”. The green synthesis of nanoparticles has the advantage of being cost-effective and eco-friendly [12]. The natural plants from which biological chelating agents can be extracted are green tea [13], lemon juice [14] and Jamun pulp [15]. During the development stages of research on the green synthesis of nanomaterials, Silva *et al.* [16] reported the use of carboxymethyl cellulose (CMC) in the synthesis of magnetic nanoparticles (MagNP-CMC). The results demonstrated good size control and yielded nanoparticles of about 10 nm. Due to the presence of CMC coating on the particles, the low saturation magnetization value ( $14.08 \text{ emu g}^{-1}$ ) obtained for the sample can be linked to its high contribution mass. Carboxymethyl cellulose-silver complex (CMC-Ag complex) had been successfully synthesized. The result showed that the chelation of silver to CMC is *via* carboxymethyl groups with the formation of a 5-membered ring and the so produced CMC-Ag particle is about 18-99 nm in size [17]. In addition, the CMC has been reported as a stabilizer and a reducing agent [18] stabilizer and immobilizer [19]. These studies suggest that CMC can be used as a chelating agent in the green synthesis of barium hexaferrite nanoparticles.

In present study, barium hexaferrite (BaF) nanoparticles are prepared by the sol-gel auto combustion method using carboxymethyl cellulose (CMC). CMC is a cellulose derivative with carboxymethyl groups ( $-\text{CH}_2\text{-COOH}$ ), which enhances the ability of chelation and water solubility. Because of its unique properties, CMC can also be used as a modifying agent in the production of nanocomposite materials [20]. Different concentrations of CMC were used for the optimization of the material preparation process. The structural, morphological and magnetic properties have been investigated employing analytical methods.

## EXPERIMENTAL

The starting compounds used were ammonium hydroxide (28-30%, Baker), barium(II) nitrate, Sigma-Aldrich), iron(III) nitrate nonahydrate (Sigma-Aldrich) and sodium carboxymethyl cellulose (CMC, Sigma Aldrich). All chemicals were of analytical grade and used without further purification in all experiments.

**Synthesis and characterization of barium hexaferrite (BaF) nanoparticles:** Initially,  $\text{Ba}(\text{NO}_3)_2$  and  $\text{Fe}(\text{NO}_3)_3 \cdot 9\text{H}_2\text{O}$  were dissolved in deionized water at a ratio of 1:12 mol under constant magnetic stirring. Then to the obtained homogeneous mixture, various concentrations (0.0, 1.0, 2.0 and 6.0% w/v) of sodium carboxymethyl cellulose (CMC) solution were added and mixed. Ammonium hydroxide solution was added dropwise to the mixture until the pH attained a value of 10. Then the solution was heated and continuously stirred at 80-100 °C for 2 h to evaporate the excess solvents. A viscous brown gel was

formed, which was eventually dried. Subsequently, the temperature was promptly increased to 200 °C. As a result, the dried gel swelled up until reaching its ignition point. Within a minute, auto-combustion occurred and has spread throughout the gel, yielding the black powder sample. X-ray diffraction (XRD) technique (Shimata, XD-D1) was used to identify the phase of the obtained sample. Scanning electron microscopy (Quanta 400, SEM-Quanta) was used to observe the microstructure of the sample. The chemical composition of the sample was analyzed using energy dispersive spectroscopy (EDS) and Fourier transform infrared (FTIR) spectroscopy techniques. The magnetization curves (M-H hysteresis loop) were measured using vibrating sample magnetometry (VSM) (Lake Shore; Model 7404). The band gap energy value of the sample was determined with the help of UV-Vis-DRS spectrophotometer (Agilent technology, Model: AL-SYS-UV-6000-M).

## RESULTS AND DISCUSSION

**XRD studies:** The effect of various concentrations of CMC on the phase composition of all samples was studied by X-ray diffraction (XRD) analysis (Philips X'PERT MPD) with CuK radiation ( $k = 1.5405$ ) in the range of  $2\theta \approx 10\text{-}90^\circ$  and at a scan rate of  $1.2^\circ$  per min. Fig. 1 shows the XRD patterns of all samples of BaF powder at different CMC concentrations, which  $\text{BaFe}_{12}\text{O}_{19}$  structure could crystallize. Interestingly, higher XRD peak intensity and lower phase formations were observed upon employing CMC as a chelating agent. As seen in Fig. 1c-d, the  $\text{BaFe}_{12}\text{O}_{19}$  phase (represented as a red star) could be formed at 2 and 6% (w/v) of CMC concentration. Citric acid is widely used in the synthesis of  $\text{BaFe}_{12}\text{O}_{19}$  [21,22]. Thus the effect of citric acid as a chelating agent was investigated and found that the XRD spectra of  $\text{BaFe}_{12}\text{O}_{19}$  exhibited characteristic main peaks at  $2\theta \approx 35^\circ, 57^\circ$  and  $64^\circ$ , which confirmed the existence of  $\text{BaFe}_{12}\text{O}_{19}$  phase in the sample [23]. Increasing the CMC concentration enhanced the formation of barium hexaferrite phase powder. On increasing the CMC concentrations from 0 to 6%, it was observed that the content of  $\text{Fe}_3\text{O}_4$  goes on decreasing while that of  $\text{BaFe}_{12}\text{O}_{19}$  increases. This shows that role of CMC is becoming increasingly beneficial for the  $\text{BaFe}_{12}\text{O}_{19}$  phase formation. The phase analysis results suggested that a minimum of 6% (w/v) of CMC is required to produce pure

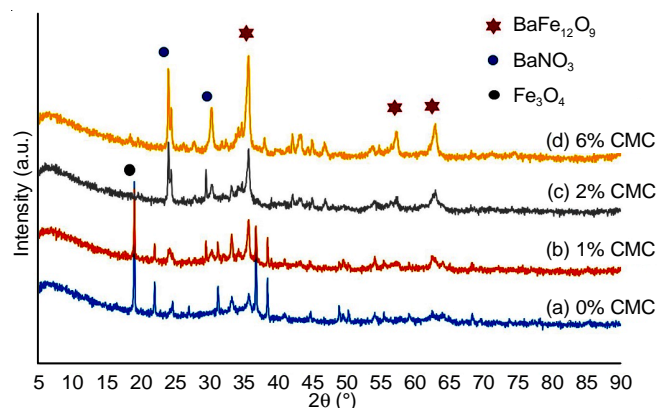


Fig. 1. XRD patterns of the obtained samples with CMC concentrations (a) 0% (w/v), (b) 1% (w/v), (c) 2% (w/v) and (d) 6% (w/v)

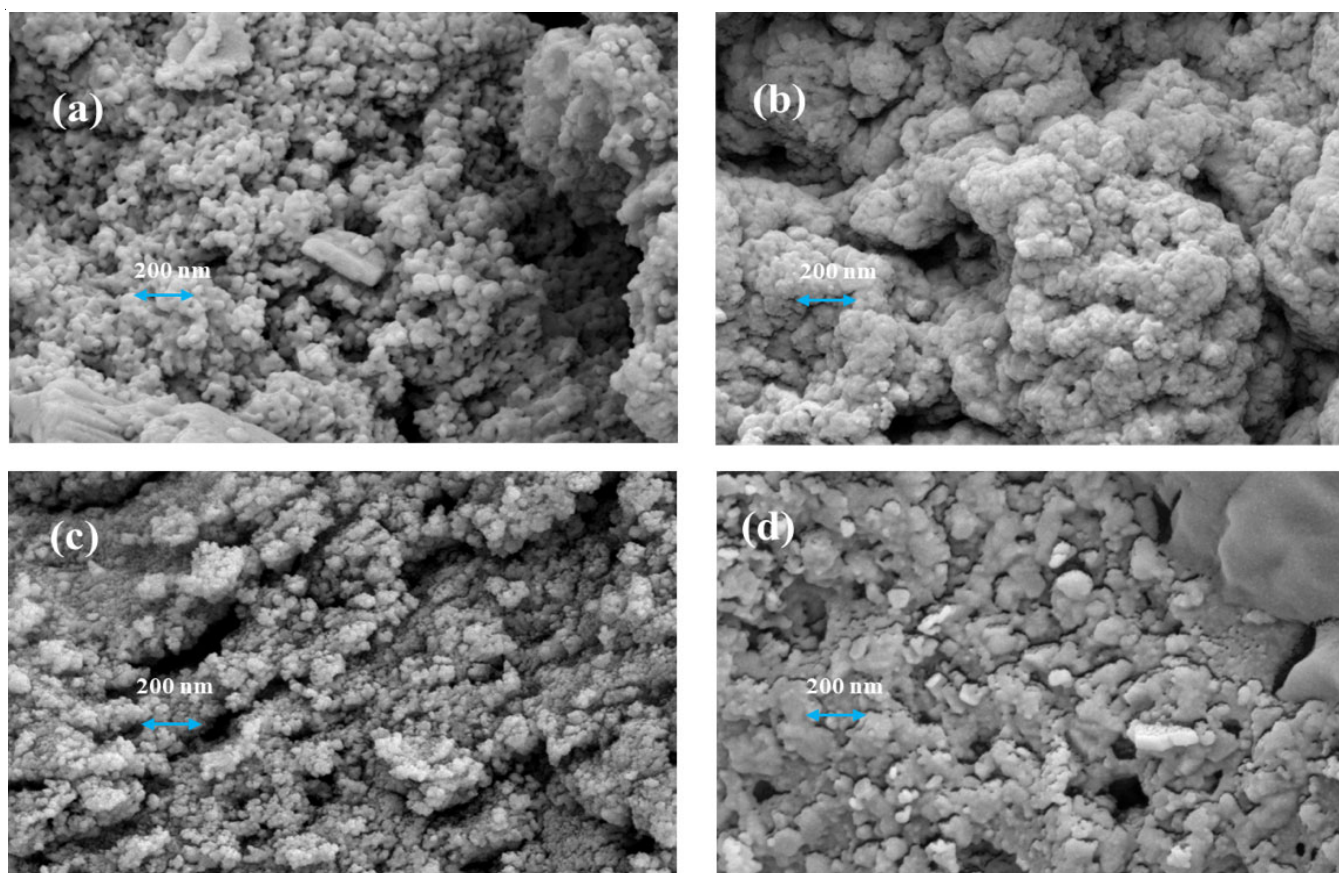


Fig. 2. SEM image of the synthesized samples with different CMC concentrations (a) 0% (w/v), (b) 1% (w/v), (c) 2% (w/v) and (d) 6% (w/v)

$\text{BaFe}_{12}\text{O}_{19}$ . The observation that BaF prepared without CMC is phase impure, whereas BaF prepared with 6% CMC gives the  $\text{BaFe}_{12}\text{O}_{19}$  phase, provides evidence for the result. This fact itself indicates that the need for low fuel, similar to what has been reported with Jamun pulp used for the synthesis of barium hexaferrite [15].

**SEM studies:** The SEM images of the samples were generated in the presence of various quantities of chelating agents. Fig. 2 displays SEM images of the obtained BaF nanoparticles at various CMC concentrations. Fig. 2a depicts the formation of granular nanoparticles in the prepared sample with 0% CMC. SEM images indicates that the particles with an average diameter of 10-15 nm are found in the samples prepared with 1, 2 and 6% of CMC concentrations (Fig. 2b-d). The morphology of the product changed from particle to thick sheet-like upon incre-asing the concentration of CMC to 6% (w/v). The formation of these obtained samples was according to Bagheri *et al.* [24] on synthesizing barium hexaferrite nanoparticles by auto-combustion using maleic acid as fuel. The effect of CMC concentration on the size of the products was investigated, since CMC could act as a chelating agent throughout the combustion reaction, leading to sphere-like particles that confirmed the crystallization of  $\text{BaFe}_{12}\text{O}_{19}$  [25].

**EDS studies:** The chemical composition and purity of  $\text{BaFe}_{12}\text{O}_{19}$  samples were evaluated through energy dispersive X-ray spectroscopy (EDS). The EDS pattern of the sample that used 6% CMC (w/v) concentration as chelating agent is

demonstrated in Fig. 3. The presence of Ba, Fe and O components in various amounts can be observed in the sample. As a result, the presence of negligible residues of impurity phases corresponding to  $\text{BaNO}_3$  and  $\text{Fe}_3\text{O}_4$  was detected in the sample. This was identified from the percentage composition of elements and the ratios of Ba, Fe and O in the sample. The EDS results were in agreement with the XRD findings.

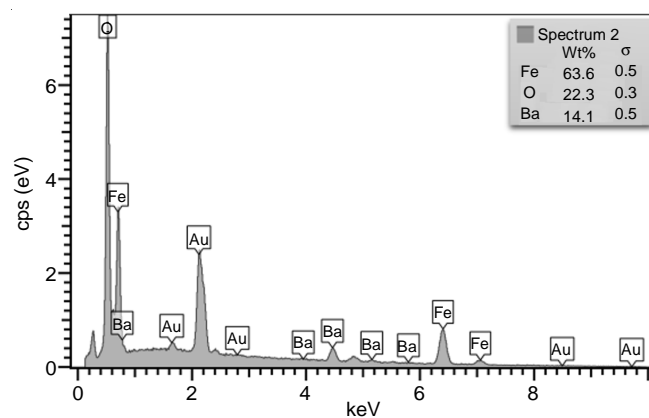


Fig. 3. EDS spectrum of  $\text{BaFe}_{12}\text{O}_{19}$  sample containing 6% (w/v) CMC concentrations

**Magnetization:** One of the most important characteristics of magnetic nanoparticles is magnetism. In a variety of practical applications, sufficient magnetic particles can swiftly

be separated from the mixture. The magnetic properties of the synthesized samples were assessed by using a vibrating sample magnetometer (VSM) in the present study. Fig. 4 shows the magnetic hysteresis loops of the obtained samples at different CMC concentrations. All BaF samples with varying levels of CMC concentrations (0, 1, 2 and 6% (w/v)) produce M-H curves with magnetization saturation values of 3.72, 4.47, 21.09 and 27.79 emu/g, respectively. The magnetization of each product increased with an increase in the concentration of CMC. The fuel content might be causing the increase in magnetization saturation. The molar fuel-to-metal-ion ratios affect the homogeneity of the metal-carboxymethyl complex's distribution in gels. This affects the gels' combustion behaviours as well as the phase compositions and magnetic characteristics of the produced barium hexaferrite powders [26].

**Band gap energy:** UV-Vis-DRS spectrophotometer was used to determine the sample's band gap energy. A complex combination of intrinsic and extrinsic features governs the overall properties of materials. The composition mostly influences an intrinsic attribute like band gap energy. Based on the band gap energy calculated, the absorption spectrum of the obtained sample shows high and low absorption bands at wavelengths in the range 200-850 nm, respectively. The band gap energy values for all the samples were calculated using a Kubelka-Munk transformation of the measured reflectance according to the equation [27]:

$$\alpha h\nu = A(h\nu - E_g)^{1/2}$$

The optical band gap of 0, 1, 2 and 6% CMC containing samples were calculated to be 1.55, 1.58, 1.60 and 1.62 eV, respectively. Fig. 5 shows that the band gap energy of BaF samples increases as the CMC concentrations rise. Several types of band gap energy loss could occur in samples, including extrinsic and intrinsic loss. Such an energy loss can be attributed to several factors, including crystal impurities, disordered

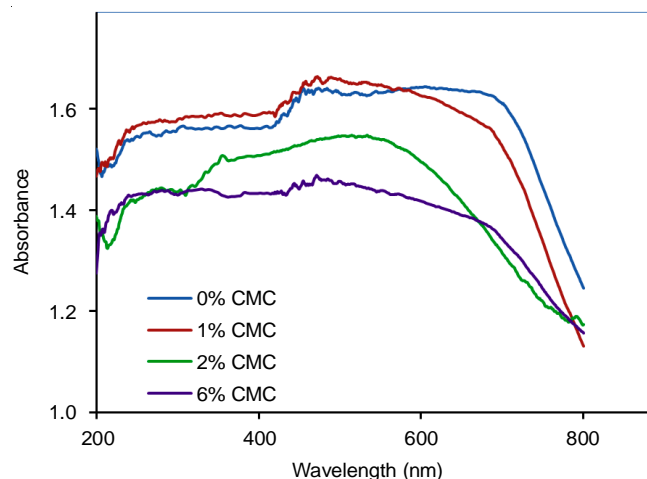


Fig. 5. UV-Vis spectrum of the synthesized samples with different CMC concentrations

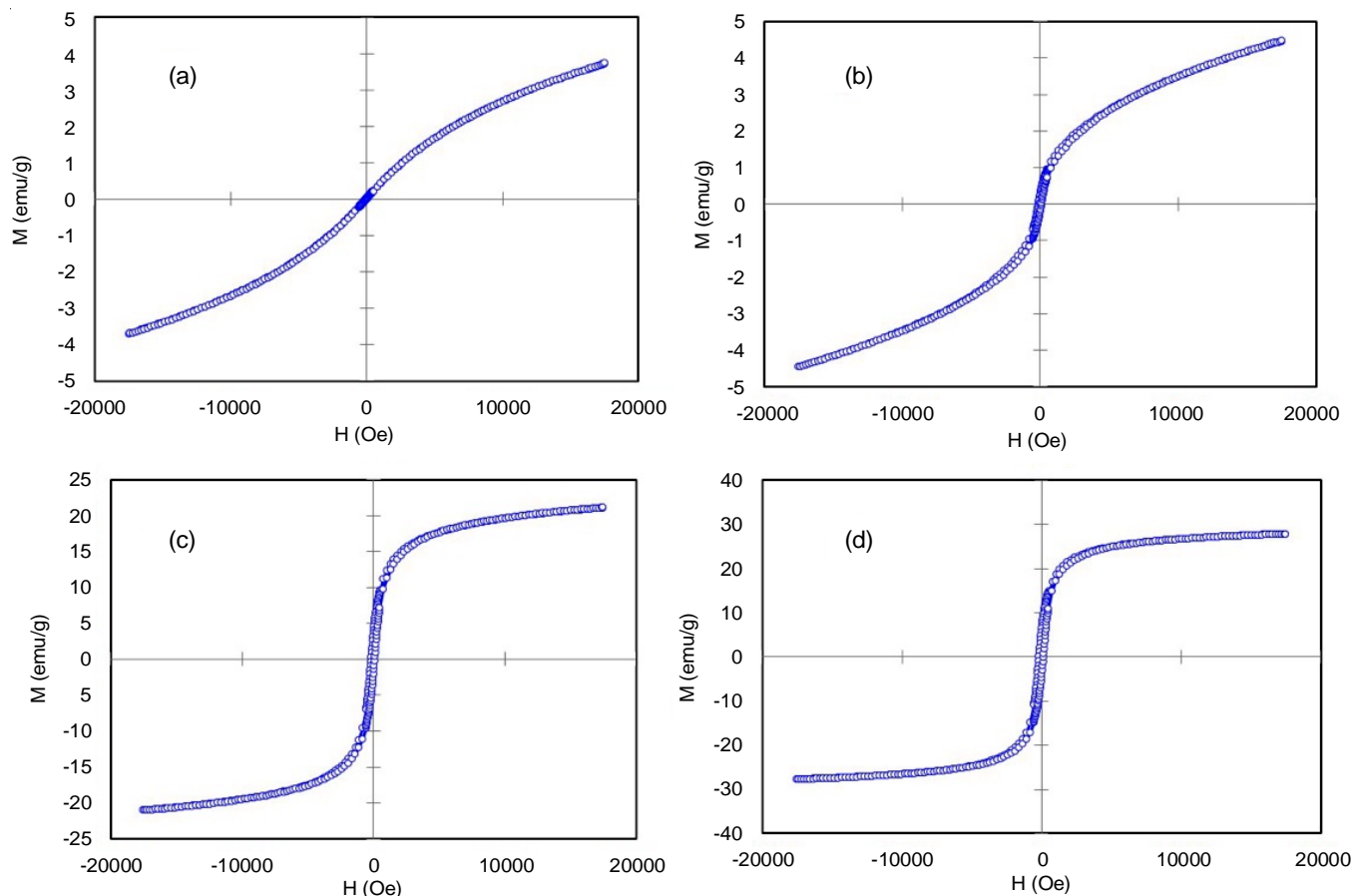


Fig. 4. M-H hysteresis loops of the synthesized samples with different CMC concentrations (a) 0% (w/v), (b) 1% (w/v), (c) 2% (w/v) and (d) 6% (w/v)

crystals and random orientation in crystalline materials [28]. The variation in their optical energy band gap with defects and interactions between the CMC and metal is responsible for the rise in energy gap values. This type of absorbance behaviour of nanocomposite samples further justifies the complexation of metal with the functional groups of CMC structures [29]. The optical energy gap's appearance can also be utilized to explain its existence and change.

**FT-IR studies:** Several characteristic bands related to CMC and  $\text{BaFe}_{12}\text{O}_{19}$  functional groups were observed in the FT-IR spectra (Fig. 6). The band corresponding to O–H stretching was visible in the CMC's IR spectrum around  $3383\text{ cm}^{-1}$ , while O–H out-of-plane vibration was seen at around  $899\text{ cm}^{-1}$ . The C=O asymmetric stretching peak was visible at  $1600\text{ cm}^{-1}$ , while the C–O bending vibration of CMC was visible at  $1600\text{ cm}^{-1}$  [30,31]. In  $\text{BaFe}_{12}\text{O}_{19}$ , the majority of Ba and Fe active modes of vibration appeared below  $400\text{ cm}^{-1}$ . The wavenumber bands in the range  $603\text{--}594\text{ cm}^{-1}$  correspond to metal–O bending vibrations in a tetrahedral shape, whereas those bands in  $1175\text{--}1020\text{ cm}^{-1}$  indicate the presence of Ba–O stretching vibrations. These correlate to the development of tetrahedral and octahedral clusters, indicating the presence of M–O stretching vibrations. The peak corresponds to Ba–O stretching is represented by the bands in the range  $900\text{--}890\text{ cm}^{-1}$  [32,33].

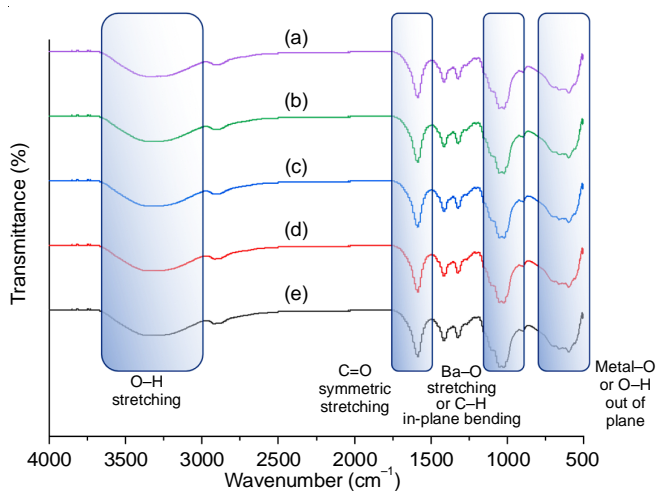


Fig. 6. FT-IR spectra of pure CMC (a) and the synthesized samples with different CMC concentrations (b) 0% (w/v), (c) 1% (w/v), (d) 2% (w/v) and (e) 6% (w/v)

## Conclusion

A low-cost approach was used to synthesize novel barium hexaferrite ( $\text{BaFe}_{12}\text{O}_{19}$ :BaF) nanocomposites. The green synthesis methodology was employed to synthesize BaF magnetic nanoparticles, which are environmentally safe, easy to fabricate and inexpensive. The structural and optical properties of the material have been investigated. The results demonstrated that utilizing carboxymethyl cellulose (CMC) as a chelating agent improved the structural and optical properties of the produced BaF sample. By increasing the concentration of CMC, the shift in the XRD peak positions has proven the presence of BaF in the composites.

## ACKNOWLEDGEMENTS

This work was supported by Creative Innovation in Science and Technology and Nanomaterials Chemistry Research Unit, Faculty of Science and Technology, Nakhon Si Thammarat Rajabhat University, Nakhon Si Thammarat, Thailand.

## CONFLICT OF INTEREST

The authors declare that there is no conflict of interests regarding the publication of this article.

## REFERENCES

- M.J. Molaei, A. Ataie, S. Raygan, S.J. Picken, E. Mendes and F.D. Tichelaar, *Powder Technol.*, **221**, 292 (2012); <https://doi.org/10.1016/j.powtec.2012.01.015>
- Y.Y. Meng, M.H. He, Q. Zeng, D.L. Jiao, S. Shukla, R.V. Ramanujan and Z.W. Liu, *J. Alloys Compd.*, **583**, 220 (2014); <https://doi.org/10.1016/j.jallcom.2013.08.156>
- T. Koutzarova, S. Kolev, Ch. Ghelev, I. Nedkov, B. Vertruen, R. Cloots, C. Henrist and A. Zaleski, *J. Alloys Compd.*, **579**, 174 (2013); <https://doi.org/10.1016/j.jallcom.2013.06.049>
- R. Hua, C. Zang, C. Shao, D. Xie and C. Shi, *Nanotechnology*, **14**, 588 (2003); <https://doi.org/10.1088/0957-4484/14/6/304>
- W. Zhong, W. Ding, N. Zhang, J. Hong, Q. Yan and Y. Du, *J. Magn. Magn. Mater.*, **168**, 196 (1997); [https://doi.org/10.1016/S0304-8853\(96\)00664-6](https://doi.org/10.1016/S0304-8853(96)00664-6)
- S. Kanagesan, S. Jesurani, M. Sivakumar, C. Thirupathi and T. Kalavani, *J. Sci. Res.*, **3**, 451 (2011); <https://doi.org/10.3329/jsr.v3i3.6483>
- T. Charoensuk, W. Thongsamrit, C. Ruttanapun, P. Jantaratana and C. Sirisathitkul, *Nanomaterials*, **11**, 558 (2021); <https://doi.org/10.3390/nano11030558>
- G. Xu, H. Ma, M. Zhong, J. Zhou, Y. Yue and Z. He, *J. Magn. Magn. Mater.*, **301**, 383 (2006); <https://doi.org/10.1016/j.jmmm.2005.07.014>
- A. Sukta and G. Mezinskas, *Front. Mater. Sci. China*, **6**, 128 (2012); <https://doi.org/10.1007/s11706-012-0167-3>
- S. Rho and S. Park, *Korean J. Chem. Eng.*, **19**, 120 (2002); <https://doi.org/10.1007/BF02706884>
- Z. Lalegani and A. Nematı, *J. Mater. Sci. Mater. Electron.*, **28**, 4606 (2017); <https://doi.org/10.1007/s10854-016-6098-5>
- P. Karpagavinayagam, A.E.P. Prasanna and C. Vedhi, *Mater. Today Proc.*, **47**, 183 (2020); <https://doi.org/10.1016/j.matpr.2020.04.183>
- X. Weng, L. Huang, Z. Chen, M. Megharaj and R. Naidu, *Ind. Crops Prod.*, **51**, 342 (2013); <https://doi.org/10.1016/j.indcrop.2013.09.024>
- Z.H. Karahroudi, K. Hedayati and M. Goodarzi, *Main Group Met. Chem.*, **43**, 26 (2020); <https://doi.org/10.1515/mgmc-2020-0004>
- S.K. Godara, R.K. Dhaka, N. Kaur, P.S. Malhi, V. Kaur, A.K. Sood, S. Bahel, G.R. Bhadu, J.C. Chaudhari, I. Pushkarna and M. Singh, *Results Phys.*, **22**, 103903 (2021); <https://doi.org/10.1016/j.rinp.2021.103903>
- D.G. da Silva, S. Hiroshi Toma, F.M. de Melo, L.V.C. Carvalho, A. Magalhães, E. Sabadini, A.D. dos Santos, K. Araki and H.E. Toma, *J. Magn. Magn. Mater.*, **397**, 28 (2016); <https://doi.org/10.1016/j.jmmm.2015.08.092>
- A.H. Basta, H. El-Saied, M.S. Hasanin and M.M. El-Defhtar, *Int. J. Biol. Macromol.*, **107**, 1364 (2018); <https://doi.org/10.1016/j.ijbiomac.2017.11.061>
- M.A. Pedroza-Toscano, S. López-Cuenca, M. Rabelero-Velasco, E.D. Moreno-Medrano, A.P. Mendizabal-Ruiz and R. Salazar-Peñ, *J. Nanomaterials*, **2017**, 1390180 (2017); <https://doi.org/10.1155/2017/1390180>

19. L.F. Greenlee and N.S. Rentz, *J. Nanopart. Res.*, **16**, 2712 (2014); <https://doi.org/10.1007/s11051-014-2712-8>
20. A. Hashim, *J. Inorg. Organomet. Polym. Mater.*, **31**, 2483 (2021); <https://doi.org/10.1007/s10904-020-01846-6>
21. A. Mali and A. Ataie, *Scr. Mater.*, **53**, 1065 (2005); <https://doi.org/10.1016/j.scriptamat.2005.06.037>
22. V.N. Dhage, M.L. Mane, A.P. Keche, C.T. Birajdar and K.M. Jadhav, *Physica B*, **406**, 789 (2011); <https://doi.org/10.1016/j.physb.2010.11.094>
23. B.C. Brightlin and S. Balamurugan, *Appl. Nanosci.*, **6**, 1199 (2016); <https://doi.org/10.1007/s13204-016-0531-1>
24. S. Mandizadeh, F. Soofivand, M. Salavati-Niasari and S. Bagheri, *J. Ind. Eng. Chem.*, **26**, 167 (2015); <https://doi.org/10.1016/j.jiec.2014.10.044>
25. S. Chanda, S. Bharadwaj, A. Srinivas, K.V. Siva Kumar and Y. Kalyana Lakshmi, *J. Phys. Chem. Solids*, **155**, 110120 (2021); <https://doi.org/10.1016/j.jpcs.2021.110120>
26. L. Junliang, Z. Wei, G. Cuijing and Z. Yanwei, *J. Alloys Compd.*, **479**, 863 (2009); <https://doi.org/10.1016/j.jallcom.2009.01.081>
27. P. Nuengmatcha, P. Porrawatkul, S. Chanthai, P. Sricharoen and N. Limchoowong, *J. Environ. Chem. Eng.*, **7**, 103438 (2019); <https://doi.org/10.1016/j.jece.2019.103438>
28. F. Bibi, S. Iqbal, H. Sabeeh, T. Saleem, B. Ahmad, M. Nadeem, I. Shakir, M. Aadil and A. Kalsoom, *Ceram. Int.*, **47**, 30911 (2021); <https://doi.org/10.1016/j.ceramint.2021.07.274>
29. M.A. Morsi, M. Abdelaziz, A.H. Oraby and I. Mokhles, *J. Mater. Sci. Mater. Electron.*, **29**, 15912 (2018); <https://doi.org/10.1007/s10854-018-9677-9>
30. M. Basuny, I.O. Ali, A.A. El-Gawad, M.F. Bakr and T.M. Salama, *J. Sol-Gel Sci. Technol.*, **75**, 530 (2015); <https://doi.org/10.1007/s10971-015-3723-3>
31. G.M. Asnag, A.H. Oraby and A.M. Abdelghany, *Compos. B. Eng.*, **172**, 436 (2019); <https://doi.org/10.1016/j.compositesb.2019.05.044>
32. S.M. El-Sayed, T.M. Meaz, M.A. Amer and H.A. El Shersaby, *Physica B*, **426**, 137 (2013); <https://doi.org/10.1016/j.physb.2013.06.026>
33. C. Thirupathy, S. Cathrin Lims, S. John Sundaram, A.H. Mahmoud and K. Kaviyarasu, *J. King Saud Univ. Sci.*, **32**, 1612 (2020); <https://doi.org/10.1016/j.jksus.2019.12.019>